

The fluorescence data in our experiments indicated that the surface coverage of the final printed layer for each of the three patterning methods presented here is nearly equivalent and reaches about 60% of the surface coverage obtained by direct deposition of the antibodies from solution. As already described for μ CP and α CP of proteins, the printing process does not compromise the binding efficiency of the printed antibody. This strategy might not be suitable for patterning a large number of different proteins on a surface. However, it can place a few different proteins as adjacent high-density arrays on a surface. Such arrays could find an application for high-throughput screening in which a large number of analytes could be spotted using a subset of the patterned areas. Another possibility for creating high-density immunoassays on planar surfaces is by performing surface immunoassays using many different analytes and capture sites, such as shown in Figure 5. The main limiting factor in using the prepared microarrays for diagnostic purposes could be misplacement of target molecules during the inking of the α -stamp. Such a misplacement, which may induce false positive reactions, can arise from cross-reactions of the target molecules with different capture proteins and/or from nonspecific adsorption on the α -stamp. The former is limited by biological specificity of affinity extraction. The latter can be limited by the systematic use of blocking agents such as BSA. Indeed, for the recognition of goat antigen by the printed array shown in Figure 5a, the recognition signal in the areas with printed anti-chicken antibodies was only 5% of that in the areas with printed anti-goat antibodies.

In summary, we have illustrated how α CP can complement different patterning methods to produce repeatedly, and in parallel, high resolution arrays of proteins in three simple steps: 1) "inking", 2) rinsing, and 3) printing the stamp on the substrate. Since α -stamps carry the complementary pattern of binding partners specific to the target proteins on their surface, the proteins self-assemble into the predefined array on the stamp surface during inking in solution, and dissociate upon printing. Hence, the (re)production of the target protein arrays is fast and easy. The initial production of the α -stamp is a one-time burden only. We thus believe that the methodology presented is powerful and versatile, and should be useful in detection and fabrication strategies that are based on arrays of proteins.

Received: January 30, 2002
Revised: April 15, 2002 [Z18619]

- [1] *Immunassay* (Eds.: E. P. Diamandis, T. K. Christopoulos), Academic Press, San Diego, CA, **1996**.
- [2] *DNA Microarrays: A Practical Approach* (Ed.: M. Schena), Oxford University Press, Oxford, UK, **1999**.
- [3] a) Y. Xia, G. M. Whitesides, *Angew. Chem.* **1998**, *110*, 568–594; *Angew. Chem. Int. Ed.* **1998**, *37*, 550–575; b) G. M. Whitesides, E. Ostuni, S. Takayama, X. Jiang, D. E. Ingber, *Annu. Rev. Biomed. Eng.* **2001**, *3*, 335–373.
- [4] A. Bernard, E. Delamarche, H. Schmid, B. Michel, H. R. Bosshard, H. Biebuyck, *Langmuir* **1998**, *14*, 2225–2229.
- [5] E. Delamarche, A. Bernard, H. Schmid, B. Michel, H. Biebuyck, *Science* **1997**, *276*, 779–781.
- [6] A. Bernard, D. Fitzli, P. Sonderegger, E. Delamarche, B. Michel, H. R. Bosshard, H. Biebuyck, *Nat. Biotechnol.* **2001**, *19*, 866–869.

- [7] C. Donzel, M. Geissler, A. Bernard, H. Wolf, B. Michel, J. Hilborn, E. Delamarche, *Adv. Mater.* **2001**, *13*, 1164–1167.
- [8] S. C. Lin, F. G. Tseng, H. M. Huang, C. Y. Huang, C. C. Chieng, *Fresenius J. Anal. Chem.* **2001**, *371*, 202–208.
- [9] A. Bernard, H. R. Bosshard, *Eur. J. Biochem.* **1995**, *230*, 416–423.
- [10] a) G. MacBeath, S. L. Schreiber, *Science* **2000**, *289*, 1760–1763; b) H. Zhu, M. Bilgin, R. Bangham, D. Hall, A. Casamayor, P. Bertone, N. Lan, R. Jansen, S. Bidlingmaier, T. Houfek, T. Mitchell, P. Miller, R. A. Dean, M. Gerstein, M. Snyder, *Science* **2001**, *293*, 2101–2105.
- [11] a) J. Hyun, A. Chilkoti, *J. Am. Chem. Soc.* **2001**, *123*, 6943–6944; b) J. S. Hovis, S. G. Boxer, *Langmuir* **2001**, *17*, 3400–3405; c) U. Schobel, I. Coille, A. Brecht, M. Steinwand, G. Gauglitz, *Anal. Chem.* **2001**, *73*, 5172–5179.
- [12] D. Juncker, H. Schmid, A. Bernard, I. Caelen, B. Michel, N. de Rooij, E. Delamarche, *J. Micromech. Microeng.* **2001**, *11*, 532–541.
- [13] E. Delamarche, A. Bernard, H. Schmid, A. Bietsch, B. Michel, H. Biebuyck, *J. Am. Chem. Soc.* **1998**, *120*, 500–508.
- [14] A. Bernard, J. P. Renault, B. Michel, H. R. Bosshard, E. Delamarche, *Adv. Mater.* **2000**, *12*, 1067–1070.
- [15] Z. Yang, A. M. Belu, A. Liebmann-Vinson, H. Sugg, A. Chilkoti, *Langmuir* **2000**, *16*, 7482–7492.
- [16] A. Bietsch, B. Michel, *J. Appl. Phys.* **2000**, *88*, 4310–4318; M. Geissler, A. Bernard, A. Bietsch, H. Schmid, B. Michel, E. Delamarche, *J. Am. Chem. Soc.* **2000**, *122*, 6303–6304.

Au-Nanoparticle Nanowires Based on DNA and Polylysine Templates

Fernando Patolsky, Yossi Weizmann,
Oleg Lioubashevski, and Itamar Willner*

The assembly of ordered nanoparticle architectures is a challenging topic in nanotechnology directed to the construction of nanoscale devices.^[1] Within this broad subject, the conjugation of biomaterials and nanoparticles to yield ordered architectures is a promising route to tailor future sensing and catalytic devices, nanocircuitry, or nanodevices, for example transistors, and computing devices.^[2] DNA is an attractive biomaterial for use as a template in programmed nanoparticle structures. The ability to synthesize nucleic acids of pre-designed shapes and composition, the versatile biocatalytic transformations that can be performed on DNA, for example, ligation, scission, or polymerization, enable "cut and paste" procedures to be carried out on the template DNA, thus enabling us to design and manipulate the DNA "mold". Furthermore, the association of metal ions to the DNA phosphate units, or the intercalation of transition-metal complexes or molecular substrates into the DNA provide a means to functionalize the DNA-template and to initiate further chemical transformations on the mold. Nanoparticle–DNA assemblies were organized by the hybridization of nucleic-acid-functionalized metal^[3] or semiconductor nano-

[*] Prof. I. Willner, F. Patolsky, Y. Weizmann, O. Lioubashevski
Institute of Chemistry
The Hebrew University of Jerusalem
Jerusalem 91904 (Israel)
Fax: (+972) 2-652-7715
E-mail: willnea@vms.huji.ac.il

particles^[4] with a complementary DNA. Metal nanowires on a template λ -DNA were generated by the initial binding of Ag^+ ions to the DNA, followed by reduction of the ions to yield catalytic sites for the electroless clustering of Ag metal on the DNA. Individual wires with a width of around 50 nm were prepared by this method.^[5] A related approach was applied to grow Pd clusters on a λ -DNA template.^[6] Similarly, CdS-nanoparticles with a positively charged modifying layer were electrostatically attracted to DNA to form a quasi-1D nanoparticle structure.^[7] Here we report a new method to generate Au-nanoparticle wires by the intercalation of psoralen-functionalized Au nanoparticles into a double-stranded DNA, followed by the photochemical covalent attachment of the intercalator with the DNA template.

Amino psoralen (**1**) was covalently-linked to 1.4-nm Au nanoparticles functionalized with a single *N*-hydroxysuccinimide group (Nanoprobes, USA; Equation (1)). (TEM experiments indicate that 5–10% of the particles exhibit a larger diameter, up to 3 nm.)

The resulting intercalator-modified Au nanoparticle was then intercalated with a double-stranded poly A/poly T duplex, of approximately 900 nm length, and the resulting assembly was irradiated with a 12 Watt UV lamp, $\lambda > 360$ nm. Under these conditions, psoralen undergoes a photoinduced $2\pi+2\pi$ cycloaddition with the thymine residues, a process that leads to the covalent attachment of the intercalator to the DNA.^[8] The obtained DNA complex was then deposited on a freshly cleaved mica surface. Figure 1 A shows the 3D AFM image of the resulting Au-nanoparticle wire. The imaged area of this wire has a length of around 600–700 nm (the wire extends beyond the imaged area) and a width of approximately 3.5–8 nm (estimated, taking into account the tip diameter, 12 nm, determined by SEM). The height of the nanowire in most of the wire domains is about 4 nm (Figure 1 B). The height of 4 nm may be attributed to the intercalation of the Au nanoparticles in a helical mode along the double-stranded perimeter of the template DNA. A few of the wire domains reach a height up to about 8 nm (Figure 1 C). These domains may originate from Au nanoparticles of larger sizes, as well as the possible bending or twisted superposition of the nanoparticle wire resulting from its deposition on the mica surface. The intercalated nanoparticles

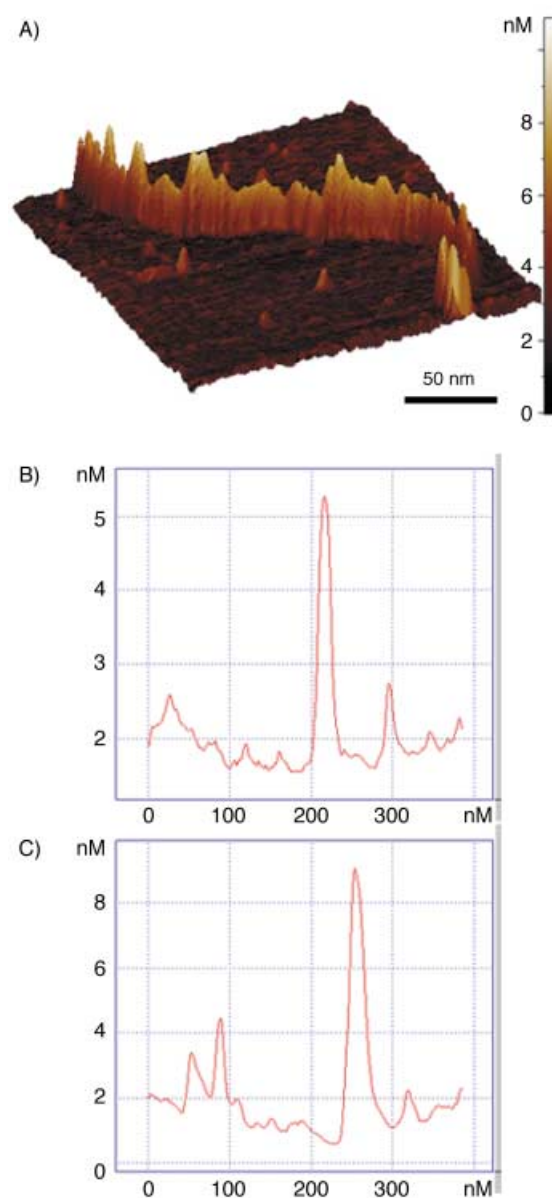
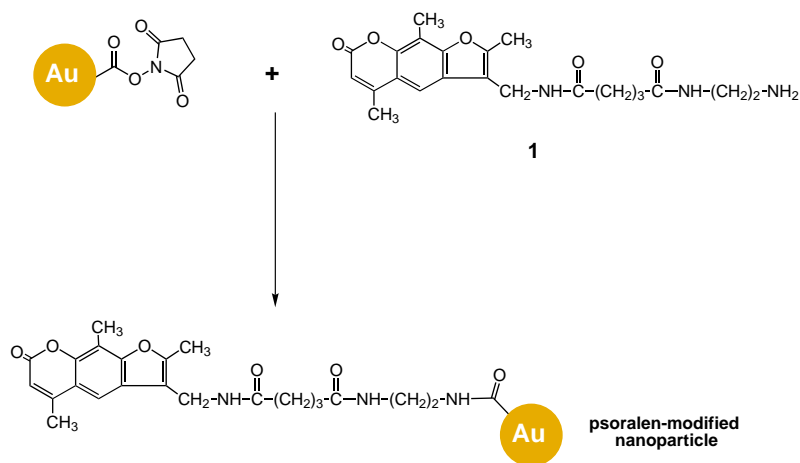


Figure 1. A) AFM image of an Au-nanoparticle wire in the poly A/poly T template. B) Cross-section of the Au-nanoparticle wire in a domain of lower height (high probability). C) Cross-section of the Au-nanoparticle wire in an area of higher height (low probability).



reveal a high-density structure in the template DNA. A similar procedure was employed to incorporate the **1**-functionalized Au nanoparticles into λ -DNA. We find that the Au-nanoparticle wires are formed, yet the density of the particles is substantially lower. Figure 2 shows the AFM image of a collection of λ -DNA templates with the incorporated Au nanoparticles. In contrast to the height observed for the Au nanoparticles incorporated into the poly A/poly T template, we find that the height of the nanoparticles incorporated into the λ -DNA, does not exceed 3.5 nm. This difference may be attributed

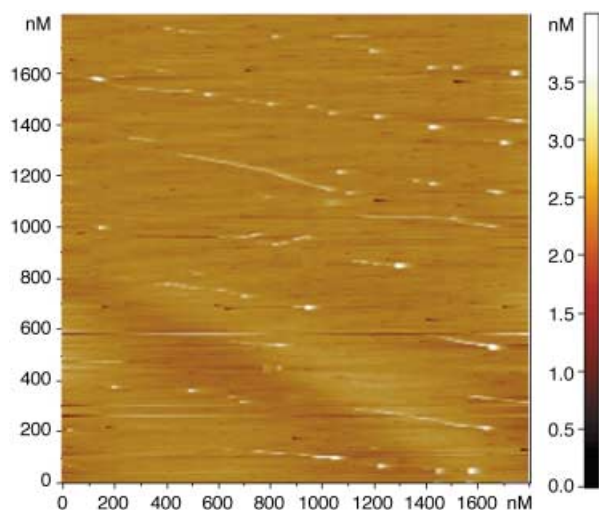


Figure 2. AFM image of Au nanoparticles incorporated in λ -DNA.

to the low-density coverage of the DNA by the particles that prevents the binding of particles on opposite sides of the surface-deposited DNA. It should be noted that the Au-nanoparticle-functionalized λ -DNA is structurally aligned on the mica surface. The alignment mechanism is not fully understood at present. Since we apply an Ar flow to dry the sample drop on the surface, it is plausible that the directional sample drying leads to the aligned structure.

A different approach to generate the Au-nanoparticle wires involves the chemical modification of poly-L-lysine with the Au nanoparticles functionalized with a single *N*-hydroxysuccinimide unit [Eq. (2)].

The deposition of the polylysine functionalized with the Au nanoparticles on a mica surface yields circular nanoparticle arrays. Figure 3 A shows the 3D structure of a circular nanowire that includes a dense assembly of Au nanoparticles. Most of the modified polylysine chains are assembled in a circular structure and no linear Au-nanoparticle wires were detected (Figure 3 B). Nonetheless, not all of the circles reveal a dense packing of the nanoparticles.

The generated circles on the mica surface reveal high stability; they are not washed off the surface with water, and they preserve their 3D structure for at least three months. Figure 3 C shows the histogram of the ring diameter of the Au-nanoparticle rings. The highest frequency is observed for rings with a diameter between 100 nm and 200 nm. A few rings reveal a small diameter of about 50 nm and some of the rings are substantially larger, around 650 nm. The polylysine employed in our study has a molecular weight of 52 000 with a dispersity of approximately 11%. This information suggests that a polymer chain includes 231 ± 25 monomer units with an average length of about 92 ± 10 nm which implies that each of the Au-nanoparticle circles is generated by several inter-

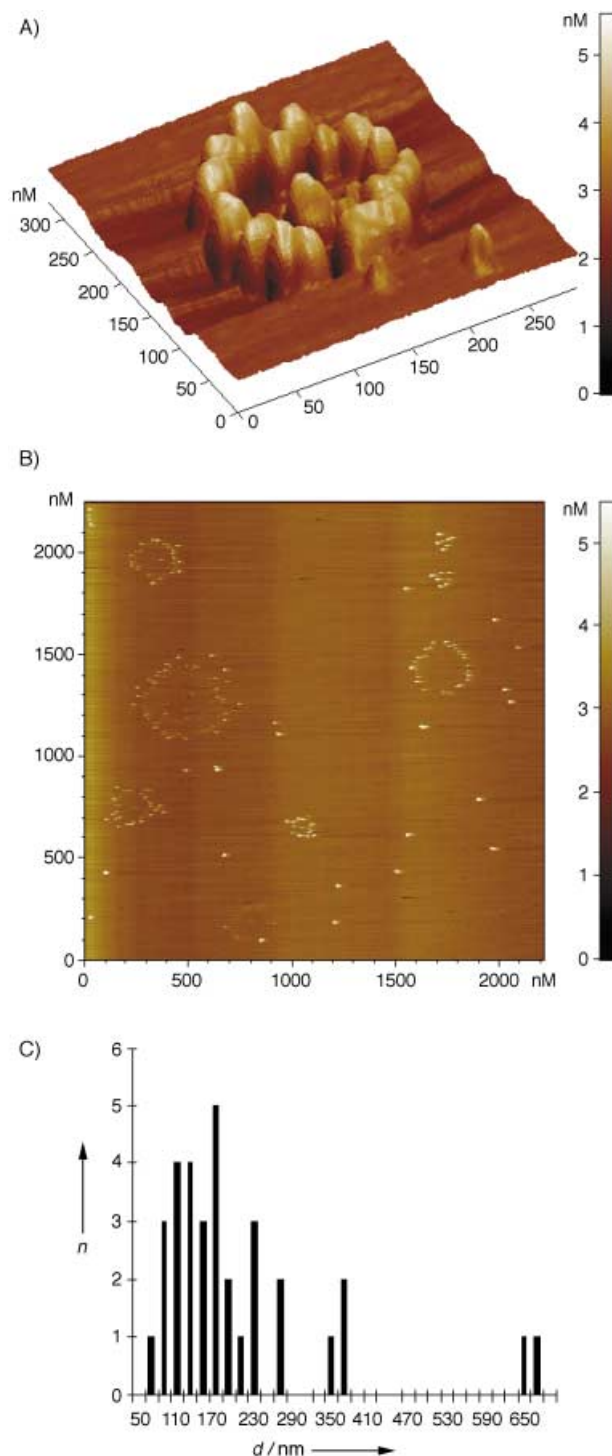
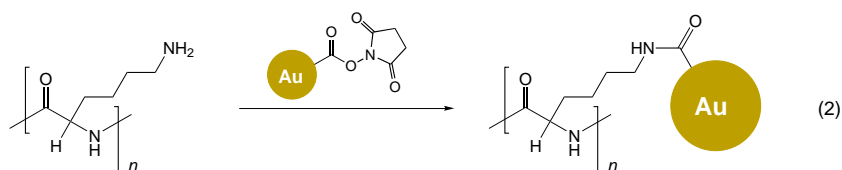


Figure 3. A) AFM image of a circular Au-nanoparticle-functionalized polylysine formed on a mica surface upon evaporation. B) Representative AFM image of Au-nanoparticle-functionalized polylysine rings formed on a mica surface upon evaporation. C) Histogram of the diameter of self-assembled Au-nanoparticle-polylysine circles on a mica surface resulting from evaporation (n = frequency; d = ring diameter).

linked polymer chains. The formation of molecular and macromolecular ring structures on surfaces has been addressed experimentally^[9, 10] and theoretically.^[11, 12] Although there is no unified theory regarding the formation of circular structures on

surfaces, based on the available knowledge, one may suggest a plausible mechanism for the formation of the Au-nanoparticle rings on the surface. The water droplet that includes the modified polylysine, wets the hydrophilic mica surface, and the film formed thins uniformly on the surface upon evaporation.^[13] When it reaches a thickness of several tenths of a nanometer, the aqueous layer reaches the point of instability, which results in film rupture and the formation of droplets. Drying of the droplets that includes the dispersed particles results in the concentration of the material at the edges of the evaporating droplet as a result of a capillary flow of the interior solution to the evaporating edges.^[11a] The diameter of the resulting ring is then controlled by the dimensions of the coalesced droplet, the number of polymer chains confined to the droplet, and the rate of evaporation that is also dominated by the concentration of the polymer in the droplet. The resulting ring is then stabilized on the mica surface by hydrogen bonds and interchain hydrogen bonds. Upon the combing^[14] of the Au-nanoparticle-functionalized polylysine on the mica surface, linear Au-nanoparticle-polymer wires are formed (Figure 4). Thus, the shape of the resulting wire can be controlled by the mode of its deposition on the surface.

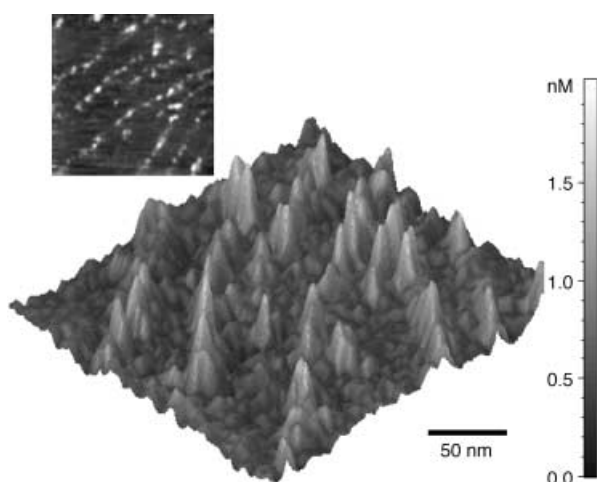


Figure 4. AFM image of Au-nanoparticle-functionalized polylysine formed on a mica surface by the combing method. Inset: 2D image of the Au-nanoparticle structures.

In conclusion, our study has demonstrated the generation of Au-nanoparticle wires on DNA or polylysine as templates. The DNA–Au-nanoparticle wires were generated by a new method that involves the incorporation of an intercalator-functionalized Au nanoparticle into double-stranded DNA, followed by the photochemical cross-linking of the intercalator to the DNA matrix. Another approach included the chemical modification of a polymer chain with the Au nanoparticles, and the surface assembly of the nanoparticle wire. The future enlargement of the nanoparticle wires by catalytic, electroless deposition of metals, is anticipated to yield conductive wires of predesigned width and shape. The future generation of conductive nanorings is particularly exciting, as it would enable the generation of nanoscale magnets by

passing a current through the nanostructures, or eventually, magnetically induced chemical reactions in nanoscale domains. Polylysine and DNA are two oppositely charged polyelectrolytes. Thus, the interaction of DNA or Au-nanoparticle-functionalized DNA with the Au-nanoparticle-tethered polylysine is anticipated to yield further nanoparticle architectures. Preliminary studies indicate that although the Au-nanoparticle rings on the mica surface exhibit high stability, their treatment with the λ -DNA that includes the intercalated Au nanoparticles results in the rupture of the Au-nanoparticle rings. We find that the Au-nanoparticle–polylysine wraps around the negatively charged DNA. This process enhances the coverage of the resulting multi-component Au-nanoparticle wires.

Experimental Section

1-Functionalized Au nanoparticles: Amino psoralen (**1**), (Sigma; 10 μ g, 40 nmol) was mixed with mono-*N*-hydroxysuccinimide-modified Au particle in a Hepes buffer solution (100 μ L; 10 mM, pH 8) for 2 h at room temperature, followed by further incubation for 12 h at 4 °C. The resulting mixture was purified from the excess of **1** using a microspin column (spin column 30, Sigma). The resulting brown solution was further dialyzed against 10 mM Hepes buffer solution using a microdialyzing device (5 kDa cutoff). All procedures were performed in the dark, to prevent photodegradation of **1**. The **1**-modified Au nanoparticles were characterized by absorption spectroscopy. From their absorption spectrum the spectrum of the pure Au nanoparticles (with the appropriate concentration factor) was subtracted to yield the absorbance band at $\lambda = 360$ nm, characteristic of **1**. From this band the concentration of **1** in the sample was determined, which gave a 1:1 ratio between **1** and the Au nanoparticles, yield 80%.

Poly-L-Lysine–Au-nanoparticle conjugate: Polylysine (52000 gmole⁻¹, 0.2 nmol) was mixed with *N*-hydroxysuccinimide-activated Au nanoparticles (6 nmol; Nanoprobes, 1.4 nm) in Hepes buffer solution (100 μ L; 30 mM, pH 8) for 12 h at 4 °C. The resulting polylysine/Au-nanoparticle conjugate was purified by spin chromatography using a gel microspin column with the appropriate fractionation range (spin column 100, >200 bases, Sigma). The resulting brown solution of the polylysine–gold-nanoparticle conjugate was further dialyzed against a Hepes buffer solution (10 mM, pH 8.5) at 4 °C for 4 h, while renewing the dialysis solution every hour, using a microdialyzing device (15 kDa cutoff).

Nanoparticle wires on surfaces: λ -DNA (Sigma) or poly A/poly T (Pharmacia) approximate 0.3×10^{-12} M concentrations were mixed with **1**-modified Au nanoparticles (1 μ m) and incubated at room temperature for 20 min. Afterwards, the mixture was irradiated with a long UV lamp (12 Watt), $\lambda > 360$ nm, for 45 min, while keeping the mixture in an ice bath. The DNA–gold-nanoparticle wires were then separated from unbound **1**–Au-nanoparticle using a microspin column of specific pore-size. A drop of the DNA-gold nanoparticle solution (4 μ L) was placed on a freshly cleaved mica surface, and allowed to evaporate. The surface was then washed with water (20 μ L) and dried with a gentle flow of argon.

The polylysine–Au-nanoparticle circles were prepared by placing a drop (4 μ L) of a 1000-fold-diluted polymer-conjugate solution (ca. 2.5×10^{-9} M) on a freshly cleaved mica surface. The drop was allowed to evaporate, and the surface was washed with triply distilled water (3×100 μ L), and dried under a gentle flow of argon. The sample could be stored for at least 3 months under an argon atmosphere.

The polylysine–Au-nanoparticle wires were prepared by the combing technique.^[14] A drop (4 μ L) was positioned on a glass surface, and this was placed on a freshly cleaved mica surface. The glass was removed and the Au-nanoparticle structures on the mica surface were imaged. Samples were imaged after 5–10 min of evaporation and gentle drying under Argon. Atomic force microscopy (AFM) images were acquired in tapping mode in air by a Smena B instrument (NT-MDT, Russia), with a 30- μ m scanner, and

NSC-16 cantilevers (resonance frequency ~ 180 kHz). Scan rates used were 1.5–2.5 Hz with a cantilever oscillation amplitude of the order of 20–40 nm.

Received: February 5, 2002 [Z18661]

A Bacterial Small-Molecule Three-Hybrid System**

Eric A. Althoff and Virginia W. Cornish*


Affinity chromatography has long been used to identify the protein targets of small-molecule drugs and other biomolecules. Although an essential tool for biochemical research, affinity chromatography can often be labor-intensive and time-consuming. Recently, the yeast three-hybrid assay, a derivative of the two-hybrid assay, was introduced as a straightforward, in vivo alternative to affinity chromatography.^[1, 2] In the three-hybrid assay, protein–small molecule interactions are detected by the dimerization of the two halves of a transcriptional activator (TA) through the receptors of the small molecule and subsequent transcription of a reporter gene.^[3–6] For affinity chromatography applications, one ligand–receptor pair is used as an anchor and the other is the small molecule–protein interaction being investigated. Although the yeast three-hybrid assay is quite powerful, a bacterial equivalent would increase the number of proteins that could be tested by several orders of magnitude because the transformation efficiency of *E. coli* is significantly greater than that of *S. cerevisiae*. Furthermore, there may be applications where it is advantageous to test a eukaryotic protein in a prokaryotic environment in which many pathways are not conserved. However, the yeast three-hybrid assay cannot be transferred directly to bacteria. The components of the transcription machinery and the mechanism of transcriptional activation differ significantly between bacteria and yeast. Ligand–receptor pairs often are organism-specific because of cell permeability, toxicity, or other interactions with the cellular milieu. Bacterial two-hybrid assays have only begun to be developed in the past few years^[7] and to date only initial efforts toward the design of a bacterial three-hybrid system have been reported.^[8, 9] Herein we report the first robust small-molecule bacterial three-hybrid system—a heterodimer of methotrexate and a synthetic analogue of FK506 that activates transcription in the *E. coli* RNA polymerase two-hybrid system (Figure 1).

We chose to construct our bacterial three-hybrid system from the RNA polymerase two-hybrid system reported by Dove et al. in 1997.^[10] A variety of methods for detecting protein–protein interactions in bacteria are now availa-

- [1] a) C. M. Niemeyer, *Angew. Chem.* **2001**, *113*, 4254–4287; *Angew. Chem. Int. Ed.* **2001**, *40*, 4128–4158; b) A. N. Shipway, E. Katz, I. Willner, *ChemPhysChem* **2000**, *1*, 18–52; c) W. Shenton, S. A. Davies, S. Mann, *Adv. Mater.* **1999**, *11*, 449–452; d) C. A. Mirkin, *Inorg. Chem.* **2000**, *39*, 2258–2272.
- [2] a) Q. H. Liu, L. M. Wang, A. G. Frutos, A. E. Condon, R. M. Corn, L. M. Smith, *Nature* **2000**, *403*, 175–179; b) E. Ben-Jacob, A. Hermon, S. Caspi, *Phys. Lett. A* **1999**, *263*, 199–202.
- [3] a) F. Patolsky, K. T. Ranjit, A. Lichtenstein, I. Willner, *Chem. Commun.* **2000**, 1025–1026; b) T. A. Taton, R. C. Mucic, C. A. Mirkin, R. L. Letsinger, *J. Am. Chem. Soc.* **2000**, *122*, 6305–6306.
- [4] I. Willner, F. Patolsky, J. Wasserman, *Angew. Chem.* **2001**, *113*, 1913–1916; *Angew. Chem. Int. Ed.* **2001**, *40*, 1861–1864.
- [5] E. Braun, Y. Eichen, U. Sivan, G. Ben-Yoseph, *Nature* **1998**, *391*, 775–778.
- [6] a) J. Richter, R. Seidel, R. Kirsch, M. Mertig, W. Pompe, J. Planschke, H. K. Schackert, *Adv. Mater.* **2000**, *12*, 507–510; b) W. E. Ford, O. Harnack, A. Yasuda, J. M. Wessels, *Adv. Mater.* **2001**, *13*, 1793–1797.
- [7] T. Torimoto, M. Yamashita, S. Kowabata, T. Sakata, H. Mori, H. Yoneyama, *J. Phys. Chem. B* **1999**, *103*, 8799–8803.
- [8] Z. Wang, K. Shah, T. M. Rana, *Biochemistry* **2001**, *40*, 6458–6464.
- [9] a) A. P. H. J. Schenning, F. B. G. Benneker, H. P. M. Geurts, X. Y. Liu, R. J. M. Nolte, *J. Am. Chem. Soc.* **1996**, *118*, 8549–8552; b) L. Latterini, R. Blossey, J. Hofkens, P. Vanoppen, F. C. de Schryver, A. E. Rowan, R. J. M. Nolte, *Langmuir* **1999**, *15*, 3582–3588.
- [10] a) S. Maenosono, C. D. Dushkin, S. Saita, Y. Yamaguchi, *Langmuir* **1999**, *15*, 957–965; b) P. C. Ohara, J. R. Heath, W. M. Gelbart, *Angew. Chem.* **1997**, *109*, 1120–1122; *Angew. Chem. Int. Ed.* **1997**, *36*, 1078–1081.
- [11] a) R. D. Deegan, O. Bakajin, T. F. Dupont, G. Huber, S. R. Nagel, T. A. Whitten, *Nature* **1997**, *389*, 827–829; b) U. Thiele, M. Mertig, W. Pompe, *Phys. Rev. Lett.* **1998**, *80*, 2869–2872.
- [12] a) D. Beaglehole, H. K. Christenson, *J. Phys. Chem.* **1992**, *96*, 3395–3403; b) A. S. Padmakar, K. Kargupta, A. Sharma, *J. Chem. Phys.* **1999**, *110*, 1735–1744; c) G. Reiter, *Phys. Rev. Lett.* **1992**, *68*, 75–78.
- [13] a) M. Elbaum, S. G. Lipson, *Phys. Rev. Lett.* **1994**, *72*, 3562–3566; b) N. Samid-Merzel, S. G. Lipson, D. S. Tannhauser, *Phys. Rev. E* **1998**, *57*, 2906–2913.
- [14] J. Hu, M. Wang, H.-U. G. Weier, P. Frantz, W. Kolbe, D. F. Ogletree, M. Salmeron, *Langmuir* **1996**, *12*, 1697–1700.

[*] Prof. V. W. Cornish, E. A. Althoff
Department of Chemistry, Columbia University
New York, NY 10027 (USA)
Fax: (+1) 212-932-1289
E-mail: vc114@columbia.edu

[**] We are grateful for financial support for this work from the National Institutes of Health (grant GM62867) and Columbia University. E.A.A. is a Howard Hughes Medical Institute Predoctoral Fellow. V.W.C. is a Beckman, Burroughs-Wellcome, Dreyfus, and NSF Career New Faculty Awardee. We especially thank A. Hochschild and S. Dove for their guidance as well as for supplying many of the plasmids and strains reported in this work; in addition, we thank Ariad Pharmaceuticals for providing a synthetic protocol for SLF and J. Hu and S. Kopytek for their many helpful suggestions.

 Supporting information for this article is available on the WWW under <http://www.angewandte.org> or from the author.